Marine Geology 335 (2013) 64–77

Contents lists available at SciVerse ScienceDirect

Marine Geology

journal homepage: www.elsevier.com/locate/margeo

Late Holocene intensification of colds fronts in southern Brazil as indicated by dune development and provenance changes in the São Francisco do Sul coastal barrier

André Zular [a,*], André O. Sawakuchi [a], Carlos C.F. Guedes [a], Vinícius R. Mendes [a], Daniel R. Nascimento Jr. [a,b], Paulo C.F. Giannini [a], Vitor A.P. Aguiar [c], Regina DeWitt [d]

[a] Departamento de Geologia Sedimentar e Ambiental, Instituto de Geociências, Universidade de São Paulo, Rua do Lago 562, São Paulo-SP, 05508-080, Brazil
[b] Departamento de Geologia, Universidade Federal do Ceará, Campus do PICI, Bloco 912, Fortaleza-CE 60455-760, Brazil
[c] Instituto de Física, Universidade de São Paulo, Rua do Matão 187, São Paulo-SP, 05508-090, Brazil
[d] Department of Physics, East Carolina University, Howell Science Complex, Rm C-209, 1000 E. 5th Street, Greenville, NC 27858, USA

ARTICLE INFO

Article history:
Received 9 August 2011
Received in revised form 20 September 2012
Accepted 14 October 2012
Available online 24 October 2012

Communicated by J.T. Wells

Keywords:
coastal barrier
aoelian dunes
OSL dating
cold fronts
Holocene climate

ABSTRACT

Holocene coastal barriers from southern Brazil present great geomorphological changes during their late stages of development. In this study, we investigate the Holocene evolution of the São Francisco do Sul (SFS) barrier through geomorphological, heavy minerals and grain size analyses constrained by Optically Stimulated Luminescence (OSL) dating. The SFS barrier stands out among the southern Brazilian barriers due to its well preserved morphology with a parabolic dune belt in the seaward portion. The progradation of the SFS barrier started at least 4914 ± 478 years ago and had a pronounced morphodynamic shift around 1891 ± 155 years ago. This shift is characterized by episodic development of parabolic dunes migrating to NNW associated with sand coarsening and a marked variation in sediment provenance represented by the input of sands derived from local coastal watersheds southward from the SFS barrier. This morphodynamic-provenance shift resulted from the strengthening of SSE winds and associated wave systems responsible for the northward alongshore drift, implying intensification of cold fronts coupled with higher precipitation since 1891 ± 155 years ago. OSL dating combined with grain size, heavy minerals and geomorphological analyses allowed assessing the response of coastal barriers to the impacts of centennial to millenial climate events occurred during the Late Holocene. Reconstruction of the Late Holocene climate variability and associated impacts on coastal sedimentation is a key issue to evaluate the sensitivity of coastal barriers to future climate changes.

1. Introduction

Beach ridges with superimposed aeolian dunes are common features of coastal sandy barriers formed by progradation of wave-dominated depositional systems following the Holocene relative sea level rise throughout the world (Clemmensen et al., 1996; Lancaster et al., 2002; Orford et al., 2003; Cooper and Navas, 2004). A great number of coastal barriers on southern Brazil prograded since the Mid-Holocene with superimposed dunes forming at later stage of barrier development (Giannini and Santos, 1994; Martinho et al., 2006; Giannini et al., 2007; Sawakuchi et al., 2008; Giannini et al., 2009; Guedes et al., 2011a, 2011b). However, the factors controlling the generation of these superimposed dunes during the later evolution stages of southern Brazilian barriers and eventual decoupling of sediments from their beach ridges and dunes have not been completely understood. The dynamics of barrier depositional systems is under the influence of climate and sea-level forcings (Cowell and Thom, 1994). Late Holocene climate changes in South America have been documented by several authors under different proxies (Rodbell et al., 1999; Haug et al., 2001; Lamy et al., 2001; Markgraf et al., 2003; Gilli et al., 2005; Wanner et al., 2008; Cruz et al., 2009; Vimeux et al., 2009; Lamy et al., 2010; Fletcher and Moreno, 2012). Despite relative sea-level playing an important role for the evolution of coastal barriers, the great geomorphological diversity of southern Brazilian barriers (Angulo et al., 2009 suggests that coastal physiography and climate are the most important forcings for their Holocene sedimentary dynamics (Sawakuchi et al., 2008; Guedes et al., 2011a); In this context, the northward migration of frontal systems (cold fronts) are particularly important for the sedimentary dynamics of coastal depositional systems in southern Brazil because it shifts and intensifies wind and wave activity (Siqueira and Machado, 2004; Rodrigues et al., 2004; Pezza and Simmonds, 2005). The activity of cold fronts in southern Brazil is sensitive to regional South American climate systems such as the westerlies wind belt (Siqueira and Machado, 2004) and the El Niño Southern Oscillation (Grimm and Doyle, 2000). Changes in the intensity and displacement

* Corresponding author at: Instituto de Geociências, Universidade de São Paulo, Rua do Lago, 562, São Paulo-SP, 05508-080, Brazil. Tel.: +55 11 3091 4128; fax: +55 11 3091 4129.
E-mail address: andrezular@gmail.com (A. Zular).

0025-3227/$ – see front matter © 2012 Elsevier B.V. All rights reserved.
http://dx.doi.org/10.1016/j.margeo.2012.10.006

of the westerlies and the onset of the El Niño Southern Oscillation (ENSO) at about 5 ka ago triggered shifts in atmospheric circulation that persist to the present day (Markgraf, 1998; Moreno, 2004; Gilli et al., 2005). The westerlies activity favors the development of frontal systems in southern South America (Stutt and Lamy, 2004; Gilli et al., 2005; Lamy et al., 2010). The northward advance of cold fronts stimulates S to SE winds as well as wave systems responsible for the northward alongshore sediment transport on the southern Brazilian coast. In this context, the São Francisco do Sul (SFS) barrier stands out as a wave-dominated prograded barrier in the southern Brazilian coast presenting well developed parabolic dunes generated by S to SE winds related to the activity of cold fronts.

The aim of this study was to evaluate the relation between aeolian dunes generation during the late stages of development of the SFS barrier and climate changes able to affect winds and waves acting on the southern Brazilian coast. Changes in sediment sources between beach ridges and superimposed dunes sands are also investigated in the SFS barrier. Variation in sediment provenance between beach ridges and adjoining coastal dunes have been reported by several authors (Bauer, 1991; Shulmeister and Kirk, 1993; Orford et al., 2003; Anthony et al., 2010) and have been associated to processes related to sea level or climate changes. Hitherto one hindrance in solving the mechanisms responsible for shifts in barrier geomorphology and sediment provenance was the lack of absolute ages. First absolute ages obtained by Optically Stimulated Luminescence (OSL) with the application of the single-aliquot regenerative-dose (SAR) protocol for beach ridges and dunes in the SFS barrier were attained. Thus, OSL ages provided a detailed chronological for sediment deposition that coupled with grain size, heavy minerals and geomorphological analyses helped to evaluate the climate significance of changes in barrier morphology and sediments provenance through time.

2. Study setting

2.1. Geological aspects

The major portion of the southern Brazilian coast rests against crystalline massifs that forms the Serra do Mar coastal range, stretching from the southern State of Espírito Santo (~20° S) to the southern portion of Santa Catarina State (~28° S, Angulo et al., 2009). Its most prominent geomorphological characteristic is the scarped coastal range that, when intersecting the coastline, creates coastal embayments where strandplains, and less frequently estuarine systems, are found (Angulo et al., 2009). The SFS barrier is located on the northern coast of the Santa Catarina State in Babitonga bay estuary vicinity (Fig. 1). It covers an area of about 280 km^2 with an approximate length of oceanic coastline of 40 km. The facing inner shelf is identified by a low-gradient slope (~0.01%) with the −50 m contour at around 45–75 km away from the shore (Angulo et al., 2009). The Precambrian substrate is composed of granitic-gneissic rocks of the Coastal Granitoid Belt (Basei et al., 1992; Siga et al., 1993). On the northernmost part of the barrier, these rocks reach the shore forming headlands and small islands. Also, they outcrop in the western part and in scattered hills throughout the barrier. Despite the occurrence of granites, low to high grade metamorphic rocks represented by schists, gneisses and migmatites (CPRM, 2004; Fig. 2B) prevail over the landward regions.

In southern Brazil, limited coastal progradation occurred in the first 1000 years after the Mid-Holocene relative sea level maximum from 7000 to 5000 years BP (Angulo et al., 2006), when the estuaries were tidal flood-dominant and sequestered sand from the coastal system (Angulo et al., 2009). Coastal progradation was accelerated first with the halt of flood dominance in the estuaries, that eventually became ebb-dominant (Angulo et al., 2009), and later by the input of abundant sediment supply that coupled with the effects of swell waves from the south and sea-level fall allowed the conditions for the progradational of a wave-dominated system and formation of the SFS barrier.

The SFS barrier is segmented by the Icaraí lagoon (Fig. 1) in western and eastern sectors, which could represent two different barriers. The western sector is up to 10 km wide and is considered by many authors (Martin and Suguio, 1975; Lessa et al., 2000; Horn Filho and Simó, 2008; Angulo et al., 2009; Possamai et al., 2010) to be a Pleistocene age barrier due to sedimentological, paleontological and geomorphological features although no chronological analysis has been undertaken yet. Its formation would be associated with the last Pleistocene relative sea-level highstand at about 120 ka, when relative sea level stood 8 ± 2 m above the present level (Martin et al., 1988). The eastern barrier is supposed to be Holocene in age and is the focus of this study. It covers an area of approximately 65 km^2 and comprises a succession of beach ridges, parabolic dunes, blowouts and established foredunes forming sand ridges with same orientation as the present coastline. All geomorphological units are composed predominantly of quartz dominated well sorted sands.

The passive Brazilian continental margin likely experienced relative tectonic stability throughout the Quaternary (Riccomini and Assumpção, 1999). Thus, it appears unlikely that tectonics have contributed to the development of Brazilian Holocene barriers. Rather, changes in the rate of sea-level variations bringing forth cycles of coastal accretion and erosion (Brunn, 1962), periods of abundant sediment supply related to episodic climatic events that affected the balance between accommodation space and sediment input have contributed to the progradation of the coastal systems and the formation of aeolian dunes in southern Brazilian barriers (Martinho et al., 2008; Sawakuchi et al., 2008; Guedes et al., 2011b). Reliable Holocene relative sea-level analyses in southern Brazil have been established through in situ carbonate vermetid shells (Angulo and Lessa, 1997; Angulo et al., 2005, 2006). Relative sea-level investigations in the Santa Catarina State show a Mid-Holocene maximum highstand of around 2.1 ± 1.0 m above present mean relative sea-level at approximately 5400–5800 cal yr BP (Angulo et al., 2006). Relative sea-level fall combined with high sediment input contribute to coastal progradation and formation of sandy barriers (Carter and Woodroffe, 1997). An overview of sea-level changes on the Brazilian coast is given by Angulo et al. (2006).

2.2. Climate

The SFS barrier climate is subtropical (Cfa, according to Koppen's classification) with wet summers and moderately dry winters. The annual rainfall varies between 1000 and 1500 mm and the mean average temperature is 18 °C. The interactions between tropical and extratropical atmospheric systems control the climate in southern Brazil (Nobre et al., 1986). The northward incursions of extratropical Polar air masses and their related cold fronts are of particular importance for the climate in southern Brazil (Seluchi and Marengo, 2000). Cold fronts migrating northward along the southern Brazilian coast occur throughout the year within 1–2 weeks intervals but they are more intense and faster during the winter (Garreaud, 1999). These cold surges provoke sudden weather changes, influencing winds and waves acting on the SFS barrier. Data collected from 1980 to 1985 indicate an average duration of a cold front from 2 to 3 days in the South Brazil Bight (Fig. 2A) with a mean time interval between successive fronts of 6.5 days (Stech and Lorenzzetti, 1992). An approaching cold front brings initially 5 m/s NE winds which may turn up to 8 m/s SSE winds during the following day. The westerlies wind belt influences the activity of the polar air mass. The position and intensity of the westerlies vary seasonally as a consequence of changes in sea surface temperature in eastern South Pacific Ocean. The westerlies belt expands northward during austral winter favoring more intense cold fronts (Heil, 2006; Lamy et al., 2010). Cold fronts can bring wet conditions to subtropical Brazil. In contrast, the warm-season precipitation (South Atlantic anticyclone) from late September to April is associated with the activity of the South American Summer Monsoon (SASM; Cruz et al., 2006; Fig. 2A). An important feature of the SASM is the South American

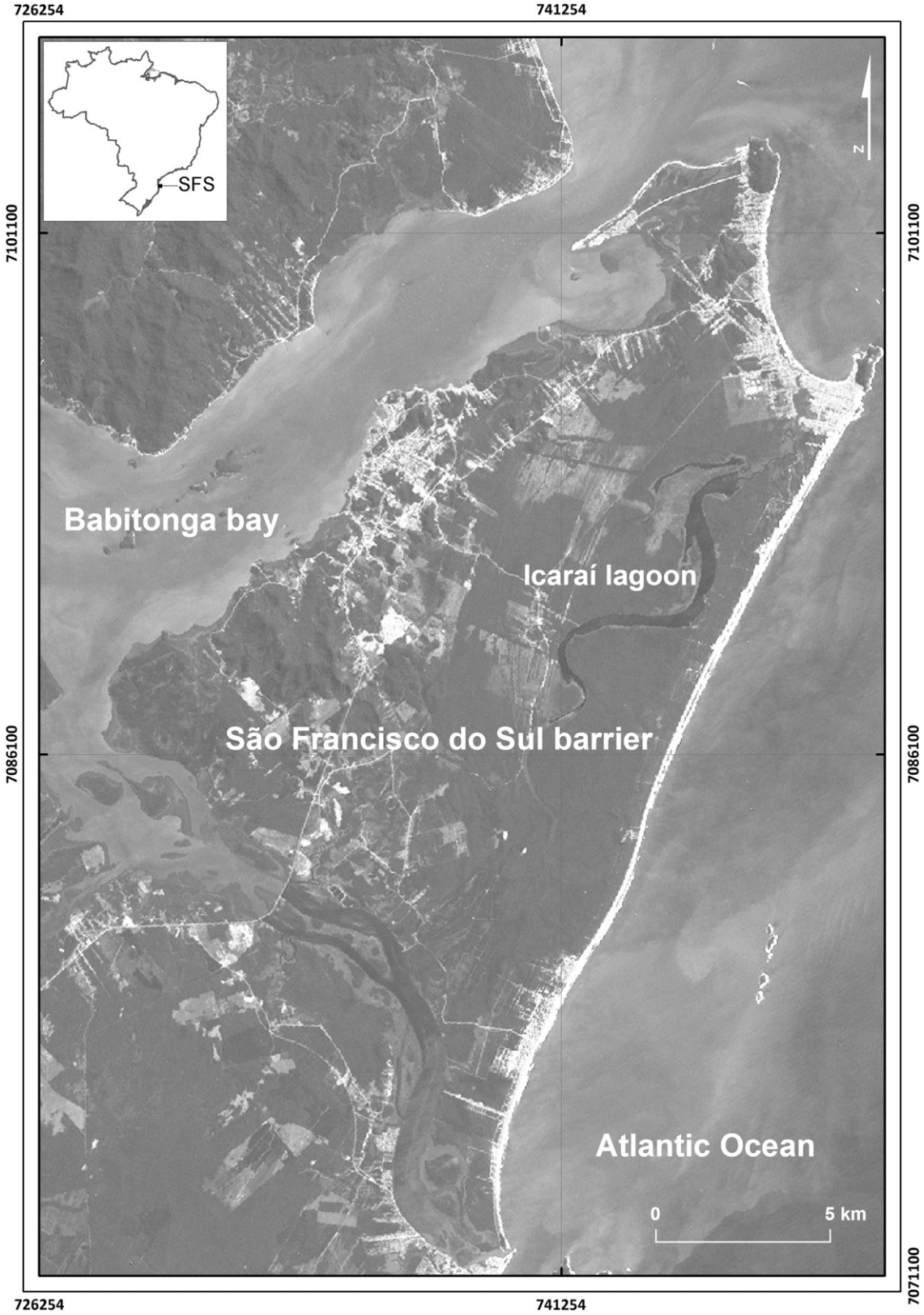

Fig. 1. Location and physiography of the São Francisco do Sul barrier (Landsat ETM +7 image, 2002).

Convergence Zone (SACZ; Fig. 2A), a NW–SE elongated band of enhanced convective activity emanating from the Amazon River basin and extending into subtropical latitudes and over the South Atlantic Coast (Cruz et al., 2006).

Usually, cold fronts associated with the northward migration of Polar anticyclones may be preceded by disturbed weather and rapid changes in wind direction. In addition, the Santa Catarina coast shows distinct interannual variations in precipitation with either

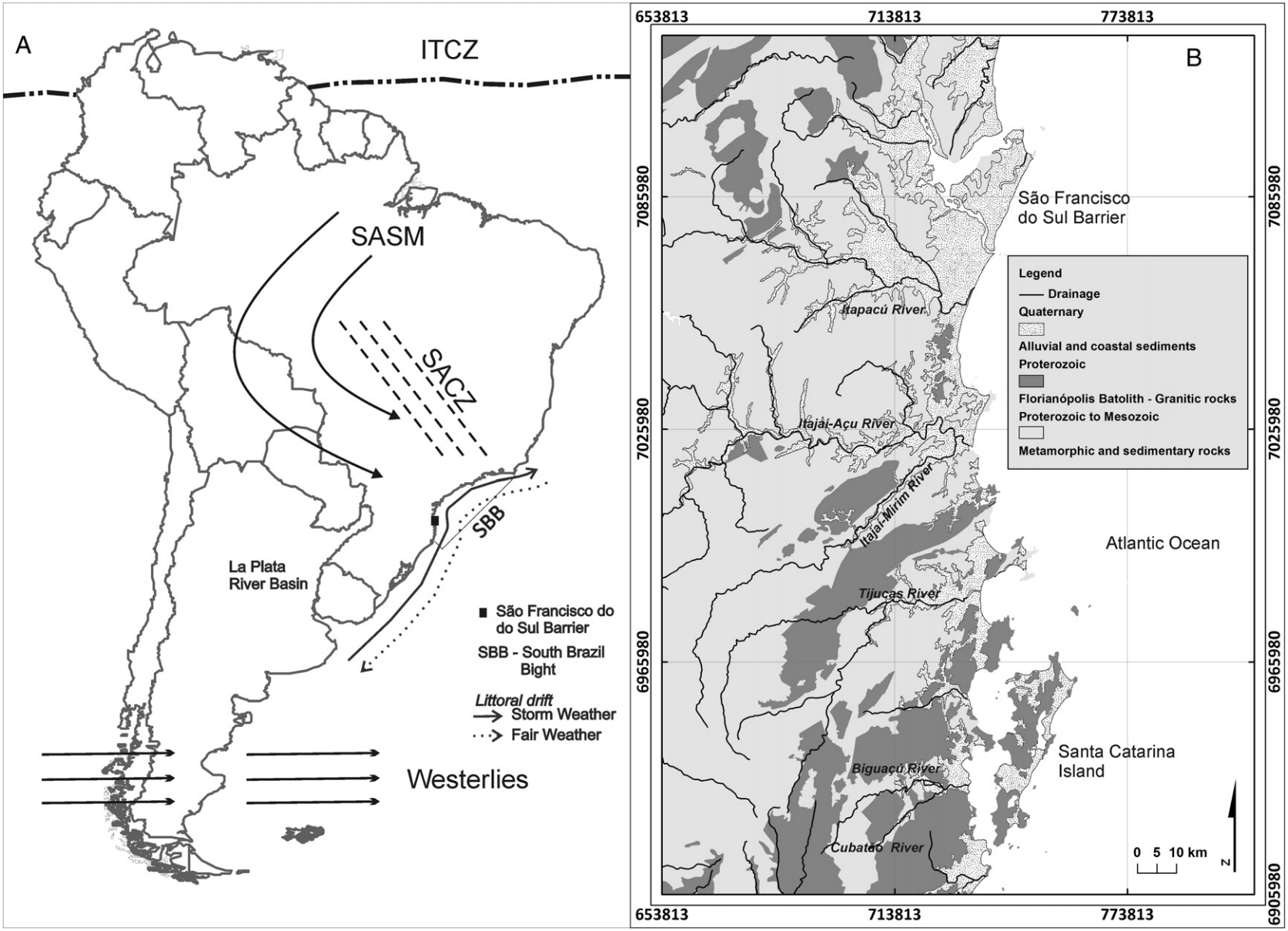

Fig. 2. A) Present-day South America climate system. ITCZ — Inter Tropical Convergence Zone; SASM — South America Summer Monsoon; SACZ — South Atlantic Convergence Zone. Climate elements based on Sylvestre (2009). B) Geological map of the eastern portion of the Santa Catarina State in southern Brazil, showing the SFS barrier. The granitic rocks south of the Itajaí-Açu River are part of the Florianópolis batholith. Major rivers and their tributaries are shown on the map. Modified from CPRM (2004).

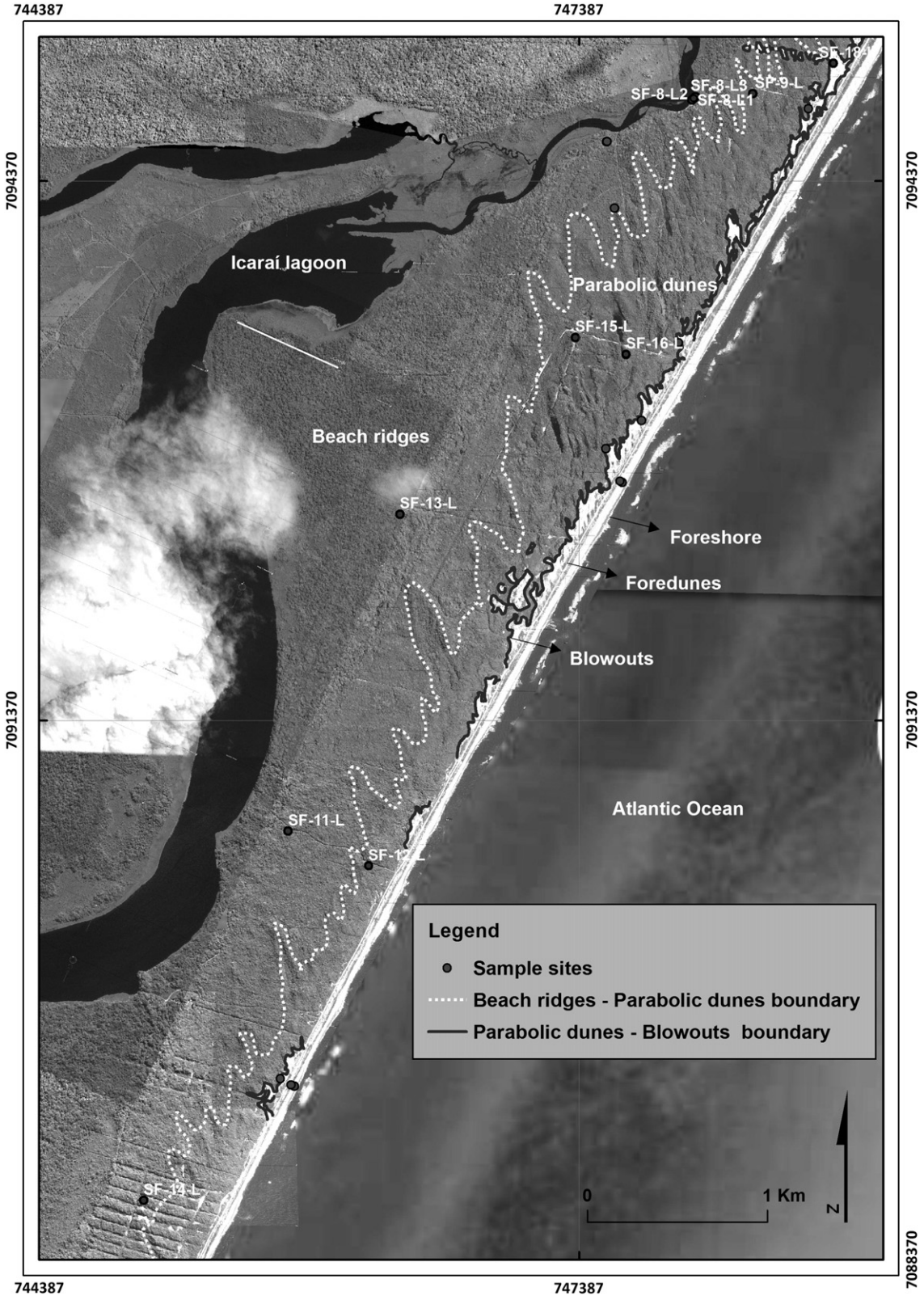

Fig. 3. Geomorphology of the São Francisco do Sul barrier showing beach ridges, parabolic dunes, blowouts, foredunes and foreshore. Dots indicate sample collection sites on the central and northern portion of the SFS barrier. OSL sampling sites are shown in white labels. OSL ages were obtained. (Google Earth image by GeoEye, 2009).

high rainfall or dry periods. This seems to be a consequence of the effect of the ENSO cycle as well as of the La Niña Southern Oscillation (LNSO) on the southern Brazil climate (Nobre et al., 1986).

The direction of more intense and predominant incident swells in the SFS barrier region is from SSE with a period of 7 to 16 s (Truccolo, 1998). Significant wave heights varying between 1 and 2 m are connected to local winds (Alves, 1996). The local tide is microtidal, mainly semidiurnal with small inequalities, with a mean range of around 0.8 m and a maximum tide level of 1.2 m (Truccolo, 1998). The meteorological influence on sea level is conspicuous. Storm

surges can raise relative sea level up to 1 m above the astronomical tide, though the relative sea level elevation may be higher when superimposed on a spring tide (Truccolo, 1998). The coastal depositional system is wave-dominated. The shore may be classified as intermediate with an exposed beach (Klein and Menezes, 2001).

Climatic variations that have occurred throughout the Mid-to Late-Holocene illustrate the frequency and magnitude of natural change within a climatic system that is similar to the present one (Milne et al., 2005). According to Cruz et al. (2006), the subtropical Atlantic coast in southern Brazil is an excellent location for investigating past changes in the atmospheric circulation because it is a region where tropical and extratropical air masses have interacted intensely during the Quaternary. Displacement of the SACZ occurred frequently during the Quaternary, usually associated with Northern Hemisphere glacial boundary conditions during Heinrich events in the Pleistocene (Cruz et al., 2007), sea surface temperature (SST) changes or Intertropical Convergence Zone (ITCZ) displacements associated with ENSO or LNSO. These changes affected the area of the SFS barrier. Fig. 2A shows the major air masses and winds currently acting in South America.

3. Methods

3.1. Geomorphology and sediment sampling

A topographic map (1:50,000), Landsat 7 and Google Earth images were used geomorphological analyses of the studied area with the help of GIS software. This enabled the identification of different depositional features and allowed planning and guidance for field surveys. Dune distribution was outlined through the analyses of satellite images and aerial photographs.

Forty five sediment samples were taken from the foreshore, foredunes, blowouts, parabolic dunes and beach ridges mostly from the eastern part of the barrier. Sample locations are shown in Fig. 3. These locations were chosen as they were expected to represent the geomorphological and sedimentological variability of the SFS barrier. Fourteen samples were collected in foreshore–foredune transects. These samples were taken along transects perpendicular to the shoreline surveying around 30 km of the coast. Sand samples were taken from the foreshore at approximately 0.5 m depth and foredune samples were taken in pits with at least 0.5 m depth on the dunes crests. Eleven sand samples from blowouts, parabolic dunes and beach ridges were taken for OSL dating. These samples were singled out to investigate the chronology of development of aeolian features and beach ridge progradation in the study area. OSL-prone samples were collected in opaque plastic tubes hammered into the sediment after cleaning the wall in outcrops or pits at a minimum of 0.5 m depth. These tubes were sealed to protect the samples from light exposure. Additional sediment samples with approximately 0.5 kg each were taken for measurement of radionuclides concentration through gamma spectrometry. The other twenty samples were collected in beach ridges and dunes of the inner portions of the barrier, aiming to assess the grain size and heavy mineral characteristics of these units.

All forty five samples were analyzed for grain-size and heavy minerals. Samples were grouped according to geomorphological units.

3.2. Grain-size analysis

Grain-size analysis was carried out in the Sedimentology Laboratory at the Universidade de São Paulo (São Paulo, Brazil). Measurements of particle-size distribution were achieved by laser diffraction method utilizing a Malvern Mastersizer granulometer with the Hydro 2000MU module. Data was tabulated in 0.125 ϕ intervals and grain-size statistics such as the mean, sorting and skewness were calculated for comparison among geomorphological units. The sediment samples were classified regarding the sorting classes proposed by Folk and Ward (1957).

3.3. Heavy-minerals analysis

Analysis of heavy minerals was performed in the very fine sand fraction. Sample preparation included elimination of the pelitic fraction through elutriation and sieving of the sand fraction to acquire the very fine sand fraction (3.75–3.25 ϕ). Heavy minerals were separated from light minerals by gravity-settling in bromoform ($CHBr_3$, density of 2.83 to 2.89 g/cm^3). Magnetic minerals were separated using a Frantz magnetic separator. The non-magnetic heavy minerals residues were mounted onto glass slides using Canada balsam for optical study under the polarizing microscope. Two hundred non-micaceous transparent heavy mineral grains plus opaque grains were computed using the ribbon counting method (Galehouse, 1971), with the content of each mineral type presented as percentage of grains within the heavy-mineral assemblage. The RZi (rutile-to-zircon ratio) provenance index as proposed by Morton and Hallsworth (1994) was measured through a dedicated count of at least 200 grains per mineral pair. The TZi (tourmaline-to-zircon ratio) was also measured using the same counting method. According to Guedes et al. (2011a), the TZi index is suitable to identify changes in patterns of sediment transport and reworking.

3.4. OSL dating

OSL dating was carried out in quartz aliquots. The samples were prepared under red light and the 3.00–2.75 ϕ or 2.75–2.50 ϕ grain size fraction was obtained by wet sieving, followed by chemical treatment with H_2O_2 27%, HCl 3.75%, HF 48–51% for 40 min, in order to remove organic carbon, $CaCO_3$, feldspars and outer rinds of quartz grains damaged by alpha particles, respectively (Aitken, 1998). Heavy minerals and remaining feldspar grains were removed through a gravity settling in lithium polytungstate solution at densities of 2.75 g/cm^3 and 2.62 g/cm^3, respectively. OSL measurements were conducted on a Risø DA-15 TL/OSL systems, in the Radiation Dosimetry Laboratory at Oklahoma State University (8 samples) and on a Risø DA-20 TL/OSL systems at the Dosimetry Laboratory of the Institute of Physics of the Universidade de São Paulo (3 samples). Both OSL readers are equipped with a Sr^{90}/Y^{90} source for beta irradiation and blue LEDs (470 nm) for OSL stimulation. The OSL was detected using Hoya U-340 filters (290–370 nm). Equivalent dose estimation was performed using the SAR protocol in quartz aliquots (Murray and Wintle, 2000; Wintle and Murray, 2006). The equivalent dose was determined by linear fitting of the dose–response data. The equivalent dose estimation of each sample corresponded to the weight mean of at least 20 quartz aliquots.

A high-purity germanium gamma-ray detector was utilized for ^{40}K, uranium and thorium estimation and determination of radiation dose rates from sediments. The samples were measured after 28 days sealed in plastic containers for radon requilibration. Beta and gamma dose rates were calculated using conversion factors outlined by Adamiec and Aitken (1998). Evaluation of cosmic rays dose rate was appraised as a function of latitude, longitude, altitude and depth below surface of the sampling point as described by Prescott and Stephan (1982). Water content for each sample was obtained as a result of differences between the total weight and dry weight after drying the sample in an oven (48 h at 110 °C). Error treatment for age calculations follows Aitken (1998).

4. Results

4.1. Geomorphology

The SFS barrier coastline orientation is around NNE. The shore exhibits occasionally berms, beach cusps and a swash zone composed of medium sand and gentle nearshore slope. It encompasses a 30–70 m wide subaerial beach. The foreshore width increases towards north,

indicating that a northward longshore sediment transport has prevailed during its development. In addition, increased beach width towards the north may also be related to a change in the beach profile from slightly convex to slightly concave in the southern portion of the barrier (Fig. 1). This can indicate a change in the sediment flow produced by waves and currents on the coast and nearshore areas, provoking more dissipative conditions northward. A narrow 5 to 10 m width belt of foredune ridges and swales occurs along the coastline. Landward, the foredunes are gradually replaced by a series of complex-shaped vegetated dunes disrupted by blowouts (Fig. 3).

Stabilized parabolic dunes superimposed to beach ridges are assembled in the central and northern part of the SFS barrier, encompassing an area of approximately 7 km^2. Many of the parabolic dunes can be classified as elongated, with length to width ratio greater than 3 (Pye, 1982). Although covered by extensive vegetation, the trailing arms are discernible and encase a central deflation corridor. Parabolic dunes in SFS barrier can reach a height of up to 17 m and up to 1 km in length. They migrate to NNW in response to the action of SSE winds. Flat lying beach ridge terrains are exposed landward from the parabolic dunes and are characterized by fine sand with low angle seaward dipping plan-parallel stratified beds. The top of parabolic dunes, blowouts and foredunes, observed in pits and trenches comprise well sorted massive medium sands.

4.2. Grain size

Grain size data was assembled by groups related to geomorphological units (Table 1; Fig. 4). Medium sand predominates in all categories, except on the beach ridges where fine sand prevails. Very fine sand is almost absent (<0.1%) on the foreshore, foredunes and blowouts notwithstanding it represents almost 8% of the beach ridges sands. Conversely, coarse sand is absent from beach ridges but it appears in considerable amounts on the other units. Very coarse sand is meaningful only on the foreshore. There is a conspicuous sand coarsening from the inner units to the outer seaward units (Fig. 4). Within the aeolian samples, parabolic dunes samples show on average approximately 0.35 ϕ finer mean diameter than foredune sands. Beach ridge sands mean diameter is around 0.60–1.20 ϕ finer than all other geomorphological units.

Table 1
Descriptive statistics of the grain size for samples grouped by geomorphological units. Q1 = first quartile, Q3 = third quartile.

	Foreshore	Foredunes	Blowouts	Parabolic dunes	Beach ridges
Mean diam (ϕ)					
Number	7	7	6	6	19
Mean	1.10	1.36	1.32	1.71	2.32
St dev	0.39	0.23	0.15	0.15	0.27
Minimum	0.61	1.12	1.04	1.51	1.87
Q1	0.83	1.15	1.33	1.60	2.18
Median	1.10	1.27	1.35	1.73	2.30
Q3	1.37	1.58	1.40	1.79	2.48
Maximum	1.62	1.63	1.46	1.92	2.86
Standard deviation (ϕ)					
Number	7	7	6	6	19
Mean	0.53	0.54	0.48	0.51	0.45
St dev	0.08	0.05	0.05	0.03	0.06
Minimum	0.45	0.48	0.40	0.47	0.37
Q1	0.48	0.51	0.48	0.48	0.40
Median	0.52	0.53	0.49	0.51	0.45
Q3	0.54	0.59	0.50	0.54	0.47
Maximum	0.68	0.60	0.54	0.55	0.57
Skewness (ϕ)					
Number	7	7	6	6	19
Mean	0.02	0.13	0.05	0.01	0.02
St dev	0.07	0.15	0.07	0.04	0.05
Minimum	−0.09	0.04	0.00	−0.06	−0.12
Q1	−0.02	0.04	0.01	0.00	0.01
Median	0.04	0.05	0.03	0.02	0.02
Q3	0.06	0.14	0.04	0.04	0.04
Maximum	0.09	0.45	0.20	0.07	0.17

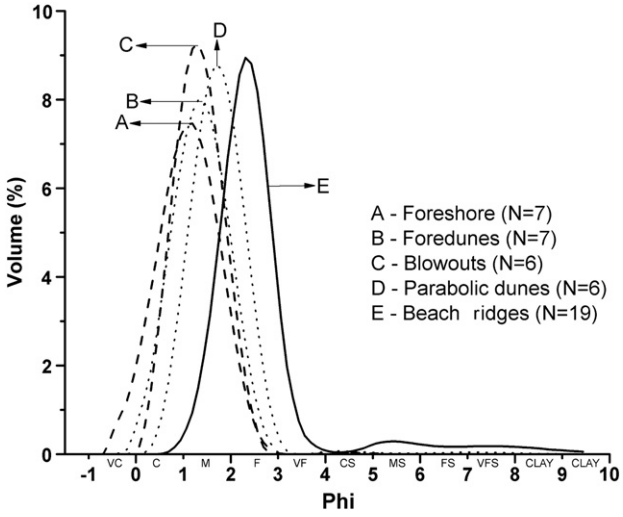

Fig. 4. Grain size distribution for each geomorphological unit (mean values). N indicates the number of samples. VC = Very coarse sand; C = Coarse sand; M = Medium sand; F = Fine sand; VF = Very fine sand; CS = Coarse silt; MS = Medium silt; FS = Fine silt; VFS = Very fine silt.

Sands from the foreshore, foredunes and parabolic dunes are more poorly sorted than those from the beach ridges and blowouts (Table 1). Sorting classes varied from well sorted (blowouts and beach ridges) to moderately well sorted (foreshore, foredunes and parabolic dunes). Overall, foreshore sands are coarser than foredune sands, though both follow the same sorting class. The grain-size distributions of all geomorphologic units are almost symmetrical as shown by skewness values near zero (Table 1). Foredune sands are on average more positively skewed than foreshore sands varying from slightly positive to negatively skewed. This trend is also observed in other barriers from southern Brazil (Amin and Dillenburgb, 2010; Guedes et al., 2011a). Pelitic material is found only on the beach ridges (Fig. 4) and could be related to more intense soil development on this sedimentary facies, since clay and silt deposition is not expected in the wave-dominated foreshore zone.

4.3. Heavy minerals

The heavy minerals concentration on the very fine sand fraction present huge variation within and among the studied geomorphological units (Table 2). A decrease in heavy mineral content is observed from SW to NE within the foreshore, foredunes and blowout units and from younger to older units, albeit some outliers were present in all geomorphological units. Table 3 shows the percentage of heavy minerals types identified in the different geomorphological units. Higher

Table 2
Heavy minerals concentration in the very fine sand fraction from different geomorphological units. N = number of samples, Q1 = first quartile, Q3 = third quartile.

% Heavy minerals	Foreshore	Foredunes	Blowouts	Parabolic dunes	Beach ridges
Number	7	7	6	6	19
Mean	63.6	43.8	57.6	34.7	6.4
St dev	26.4	15.8	8.9	9.0	8.1
Minimum	28.2	23.7	46.1	23.8	0.4
Q1	41.0	32.5	53.9	27.1	1.2
Median	71.7	45.5	57.3	36.1	4.5
Q3	83.9	54.9	58.6	40.6	7.8
Maximum	95.4	62.6	73.2	45.8	30.4

Table 3
Percentage of heavy minerals (mean values) identified in the geomorphological units from the SFS barrier. N = number of samples, Zi = Zircon, Tu = Tourmaline, Ru = Rutile, Hn = Hornblende, Ep = Epidote, Sl = Sillimanite, Ky = Kyanite, St = Staurolite, Mz = Monazite, Hy = Hypersthene, Di = Diopside, Gr = Garnet, Ap = Apatite, Cl = Clinozoisite, Ac = Actinolite, Tr = Tremolite, An = Andaluzite, En = Enstatite.

Unit	Stats	Zi	Tu	Ru	Hn	Ep	Sl	Ky	St	Mz	Hy	Di	Gt	Traces
Foreshore	Mean (%)	77.8	Tr	1.2	4.4	8.4	Tr	Tr	1.1	Tr	1.3	0.0	1.5	Ap, Cl,
N = 7	Std dev	13.5	0.8	1.0	3.0	6.0	1.3	0.9	1.3	1.5	1.3	0.0	3.4	Ac
Foredunes	Mean (%)	73.4	1.3	1.4	7.9	9.3	1.3	Tr	1.0	1.0	1.8	Tr	Tr	Cl, Ac
N = 7	Std dev	10.1	1.2	0.6	4.7	5.3	1.0	0.9	0.9	1.1	0.9	0.2	0.4	
Blowouts	Mean (%)	75.3	1.8	1.7	7.5	7.4	Tr	Tr	1.1	Tr	2.5	0.0	Tr	Cl, Tr,
N = 7	Std dev	8.3	1.0	0.8	4.5	3.6	0.4	0.6	0.9	1.1	1.7	0.0	0.2	An, Ac
Parabolic dunes	Mean (%)	72.0	3.1	2.3	8.0	7.3	1.0	Tr	1.8	Tr	2.3	0.0	Tr	An, Ac,
N = 6	Std dev	13.6	2.8	1.5	6.0	4.0	0.9	0.3	1.5	0.6	2.1	0.0	0.5	En
Beach ridges	Mean (%)	58.4	9.4	11.7	2.8	4.9	3.2	6.1	1.9	Tr	Tr	0.0	0.0	Cl, An,
N = 19	Std dev	22.9	9.1	7.6	7.8	8.7	3.3	5.1	2.0	0.1	0.5	0.0	0.0	Ac, En

concentrations of rutile, kyanite, sillimanite and staurolite point to a metamorphic-dominated provenance of the beach ridge sediments. In turn, all other units show higher contents of zircon and hornblende, suggesting a greater contribution of sediments derived from igneous rocks. However, intermixing occurs in both assemblages. Zircon is present in all samples although older deposits showed a relatively low content of zircon (Table 4). Sediments from the beach ridges compared to all other geomorphological units stand out due to the great difference between the shapes of their zircon grains. Zircon grains from the beach ridges are rounded to sub-rounded in contrast to more euhedrical to subeuhedrical forms found in the other units (Fig. 5).

Table 5 shows the statistics of RZi and TZi on the studied barrier. A conspicuous association between geomorphological units and the RZi can be observed. The beach ridges present higher RZi values. The same E–W increase trend observed in the RZi is displayed in the TZi. This indicates that provenance is the major control on the variation of TZi within the SFS barrier.

4.4. OSL ages

The equivalent dose, dose rate and OSL ages are shown on Table 6. The dose response curves for all aliquots follow a linear trend (Fig. 6A). The equivalent dose distributions of all dated samples presented low dispersion, suggesting well bleaching and absence of sediment mixing throughout the profile (Fig. 6C and D). Recycling ratios vary from 0.9 to 1.1 in 99% of the measured aliquots with a mean of 0.99 (N = 252), connoting that sensitive changes had been corrected adequately (Fig. 6B). These characteristics attest to a reliable OSL age determination. The OSL ages range from 87 ± 8 to 4914 ± 478 years (Table 6) with errors from 8% to 11%, covering the Mid- to Late Holocene.

The OSL dates follow an expected temporal progression based on their geomorphological positions, indicating a prograding coast. This chronology supports a depositional model of wave-dominated beach ridges progradation followed by the development of superimposed aeolian dunes in some locations. Beach ridges without or with limited dune cover are older than 3321 ± 287 years whereas parabolic dunes show ages younger than 1891 ± 155 years (Table 6; Fig. 7). Recently reactivated blowouts are located close to foredunes (Fig. 8) or parabolic dunes lying less than 200 m from the foreshore. All beach ridges ages are consistent with a sediment accumulation in a progradational coast, with ages decreasing from base to top in vertical profiles and seaward in horizontal transects. The only age inversion was observed in sample SFS-8-L2, when compared to sample SFS-8-L1. These two samples were taken from the same unit apparently representing equal depositional facies. OSL ages for SFS-8-L1 (bottom layer) and SFS-8-L2 (top layer) were 3104 ± 305 and 4541 ± 454 years, respectively. This apparent age inversion possibly indicates dose rate changes caused by sediment leaching after burial (Madsen and Murray, 2009). Incomplete bleaching and sediment mixing are unreliable due to narrow equivalent dose distributions. In this case, the dose rate of the top layer would be underestimated due to leaching of minerals enriched in radionuclides. On the other hand, the bottom layer would have an overestimated dose rate due to the concentration of radionuclides derived from the upper layer. This is also supported by the higher equivalent dose presented by the bottom layer (sample SFS-8-L1).

Table 4
Percentage of zircon grains in the different SFS barrier geomorphological units. Q1 = first quartile, Q3 = third quartile.

Zircon	Foreshore	Foredune	Blowouts	Parabolic dunes	Beach ridges
Number	7	7	6	6	19
Mean	77.8	73.4	75.3	72.0	58.4
St dev	13.5	10.1	8.3	13.6	22.9
Minimum	57.4	59.2	66.0	56.9	11.1
Q1	71.2	67.5	68.9	62.5	46.7
Median	82.1	72.5	75.6	72.2	61.7
Q3	84.5	78.4	79.0	75.1	76.0
Maximum	93.8	90.1	88.0	95.1	88.0

5. Discussion

5.1. Barrier progradation and aeolian dune building

The oldest beach ridge age obtained for the SFS barrier was 4914 ± 475 years, suggesting that barrier progradation began during the Mid-Holocene, around the relative sea-level maximum between 7000 and 5000 years cal BP in the Brazilian coast (Angulo et al., 2006). The beginning of progradation of the SFS barrier is approximately synchronous to the progradation of the Ilha Comprida barrier, which started at around 6041 ± 504 years ago (Guedes et al., 2011b). The Ilha Comprida barrier is located 145 km to the north of the SFS barrier, suggesting that relative sea level stabilization was a trigger for barrier progradation in southern Brazil. The progradation of the SFS barrier occurred under two modes of deposition. The first mode that comprised the period from 4914 ± 475 to at least 3321 ± 287 years ago encompasses beach ridges formation without significant dune building. This period marks the onset of significant sediment accumulation in the wave-dominated coastal system, with barrier progradation and coastline regression. The progradation during this phase occurred under a sea level fall of 1.5 m, with progradation rates varying from 0.1 to 0.6 m/year on the shore-normal direction. The highest progradation rates were found on the north-central part of SFS barrier. The range of progradation rates obtained for the SFS barrier is similar to those obtained for the Ilha Comprida barrier (Guedes et al., 2011b) and other Holocene barriers worldwide, as Guichen Bay, South Australia (Murray-Wallace et al., 2002; Bristow and Pucillo, 2006). The development of impressive parabolic dunes covering wave-dominated beach ridges marks the shift in the mode of progradation of the SFS barrier. The oldest OSL ages determined for these parabolic dunes were 1891 ± 155 years (sample SFS-9-L) and 1881 ± 182 years (sample SFS-12-L). Sample site SFS-12-L is located only 130 m from the beach ridges–parabolic

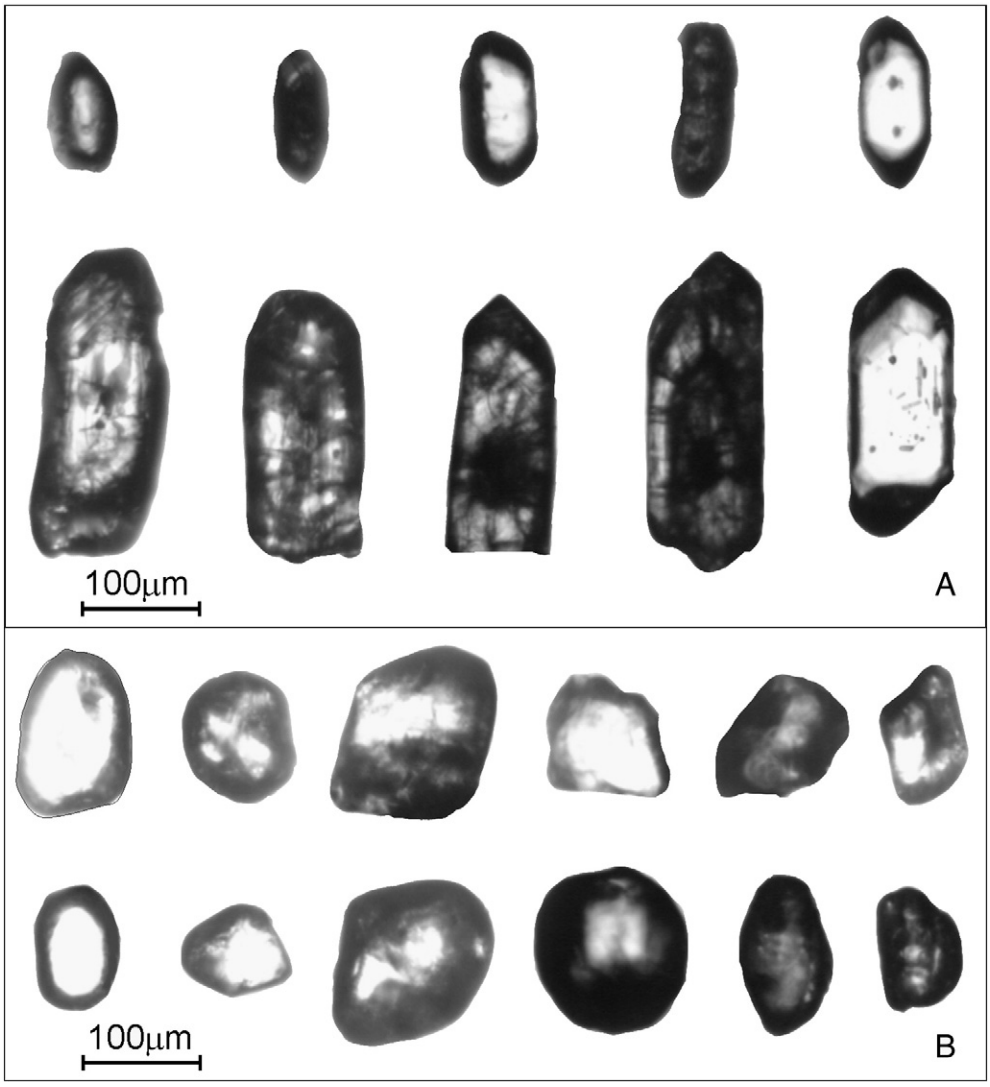

Fig. 5. A) Zircon grains from parabolic dunes, blowouts, foredunes and foreshore sands. B) Zircon grains from beach ridge sands.

dunes boundary (Fig. 3). It should then be expected that the age of 1891 ± 155 years represents the beginning of parabolic dunes emplacement on the SFS barrier. The parabolic dunes of the SFS barrier are elongated, with lobes pointing to NNW, long arms and narrow deflation basin. This parabolic dune morphology attests to higher wind speeds as suggested by Gaylord and Dawson (1987) in studies of airflow–terrain interactions., Blowout formation may be linked to periods of increased storminess, high speed wind erosion and climate change (Hesp, 2002). Blowouts may evolve in various ways, depending on wind speeds, dominant wind direction, vegetation types, sand supply, magnitude and occurrence of beach/dune erosion and storm events, barrier/beach status and vegetation damage due to human activities (Hesp, 2002). In the course of time, many blowouts may become sizable and evolve into parabolic dunes (Carter and Woodroffe, 1997). The dune development in the SFS barrier since 1891 ± 155 years ago represents an abrupt increase in the activity of SSE winds. In contrast, blowouts and foredunes developed in the last 87 years ± 8 years mark a change to a period of relatively lower wind activity, albeit stronger than during the phase dominated by beach ridges progradation.

The SFS barrier sands become coarser at the onset of formation of aeolian dunes (Fig. 4). Beach ridges are dominated by very fine sand while parabolic dunes, blowouts, foredunes and the foreshore comprise mainly medium to coarse sand. The foreshore stands out to include the highest proportion of coarse sand (Fig. 4). This huge shift

Table 5
Values of RZi and TZi from different geomorphological units from the SFS barrier. Q1 = first quartile, Q3 = third quartile.

Rzi	Foreshore	Foredune	Blowouts	Parabolic dunes	Beach ridges	Tzi	Foreshore	Foredune	Blowouts	Parabolic dunes	Beach ridges
Number	7	7	6	6	19	Number	7	7	6	6	19
Mean	1.5	1.6	2.1	2.9	18.1	Mean	0.8	1.9	2.1	4.9	15.7
St dev	1.2	0.8	0.9	1.4	9.9	St dev	0.9	1.6	0.9	4.1	18.1
Minimum	0.5	0.9	1.0	1.0	5.0	Minimum	0.0	0.0	1.2	0.0	0.0
Q1	0.6	1.0	1.4	2.0	7.8	Q1	0.0	0.9	1.4	2.6	3.2
Median	1.0	1.4	2.2	2.8	21.1	Median	0.7	1.9	1.7	4.5	6.4
Q3	2.3	2.0	2.8	4.1	26.2	Q3	1.2	2.4	2.7	6.0	24.9
Maximum	3.3	3.0	3.3	4.7	35.7	Maximum	2.4	4.9	3.4	11.8	57.1

Table 6
OSL dating results from beach ridges, parabolic dunes and blowouts from the SFS barrier.

Sample	X (UTM)	Y (UTM)	Unit	Aliquots	Dose (mGy)	K (%)	Th (ppm)	U (ppm)	Total dose rate (mGy/year)	Gama dose rate (mGy/year)	Beta dose rate (mGy/year)	Cosmic dose rate (mGy/year)	Age (years)
SFS-18-L	748801	7095029	Blowout	24	76 ± 4	0.341	4.025	0.328	0.880 ± 0.066	0.301 ± 0.0037	0.378 ± 0.054	0.2015 ± 0.0101	87 ± 8
SFS-8-L3	748034	7094844	Parabolic dune	24	1366 ± 58	0.328	3.623	0.156	0.787 ± 0.063	0.257 ± 0.038	0.333 ± 0.049	0.1971 ± 0.0099	1735 ± 158
SFS-9-L	748352	7094860	Parabolic dune	24	1949 ± 83	0.233	7.008	0.59	1.030 ± 0.072	0.437 ± 0.049	0.392 ± 0.052	0.2017 ± 0.0101	1891 ± 155
SFS-12-L	746217	7090565	Parabolic dune	24	1214 ± 52	0.347	1.45	0.115	0.646 ± 0.056	0.158 ± 0.032	0.294 ± 0.045	0.1934 ± 0.097	1881 ± 182
SFS-15-L	747367	7093504	Parabolic dune	20	1063 ± 46	0.379	3.881	0.388	0.875 ± 0.065	0.304 ± 0.035	0.402 ± 0.055	0.1689 ± 0.0084	1215 ± 105
SFS-16-L	747649	7093410	Parabolic dune	24	1505 ± 68	0.287	6.227	0.48	1.001 ± 0.100	0.400 ± 0.078	0.400 ± 0.062	0.2014 ± 0.0101	1503 ± 165
SFS-11-L	745770	7090759	Beach Ridge	24	3583 ± 153	0.24	6.8	0.858	1.079 ± 0.081	0.453 ± 0.056	0.421 ± 0.058	0.2048 ± 0.0102	3321 ± 287
SFS-14-L	744968	7088705	Beach Ridge	24	2024 ± 87	0.213	1.976	0.243	0.589 ± 0.055	0.162 ± 0.222	0.222 ± 0.04	0.2046 ± 0.0102	3439 ± 354
SFS-13-L	746392	7092520	Beach Ridge	20	7472 ± 337	0.2	12.199	1.476	1.521 ± 0.130	0.743 ± 0.104	0.574 ± 0.078	0.2038 ± 0.0102	4914 ± 475
SFS-8-L1	748014	7094824	Beach Ridge	24	2893 ± 124	0.656	1.598	0.401	0.932 ± 0.082	0.267 ± 0.037	0.557 ± 0.074	0.1079 ± 0.0054	3104 ± 305
SFS-8-L2	748024	7094834	Beach Ridge	20	2140 ± 96	0.271	0.762	0.207	0.471 ± 0.042	0.118 ± 0.018	0.235 ± 0.038	0.118 ± 0.0059	4541 ± 454

in grain size since aeolian dune building is abrupt and surpasses grain size variations related to alongshore drift as observed in other southern Brazilian barriers (Guedes et al., 2011a). This suggests lower wind and wave energy during the phase dominated by beach ridges progradation in relation to the phase with dune building. Thus, the formation of aeolian dunes in the SFS barrier would be coupled to a rapid energy increase of waves and associated currents responsible for the sand input to the barrier. Also, parabolic dunes migration and stabilization between 1891 ± 155 and 1215 ± 105 years ago imply relatively wet climate, but under a SSE wind regime able to provide episodes of dune movement.

5.2. Changes in sediment provenance

The heavy minerals of the SFS barrier sands comprise two different assemblages. Beach ridges sands are enriched in heavy minerals from

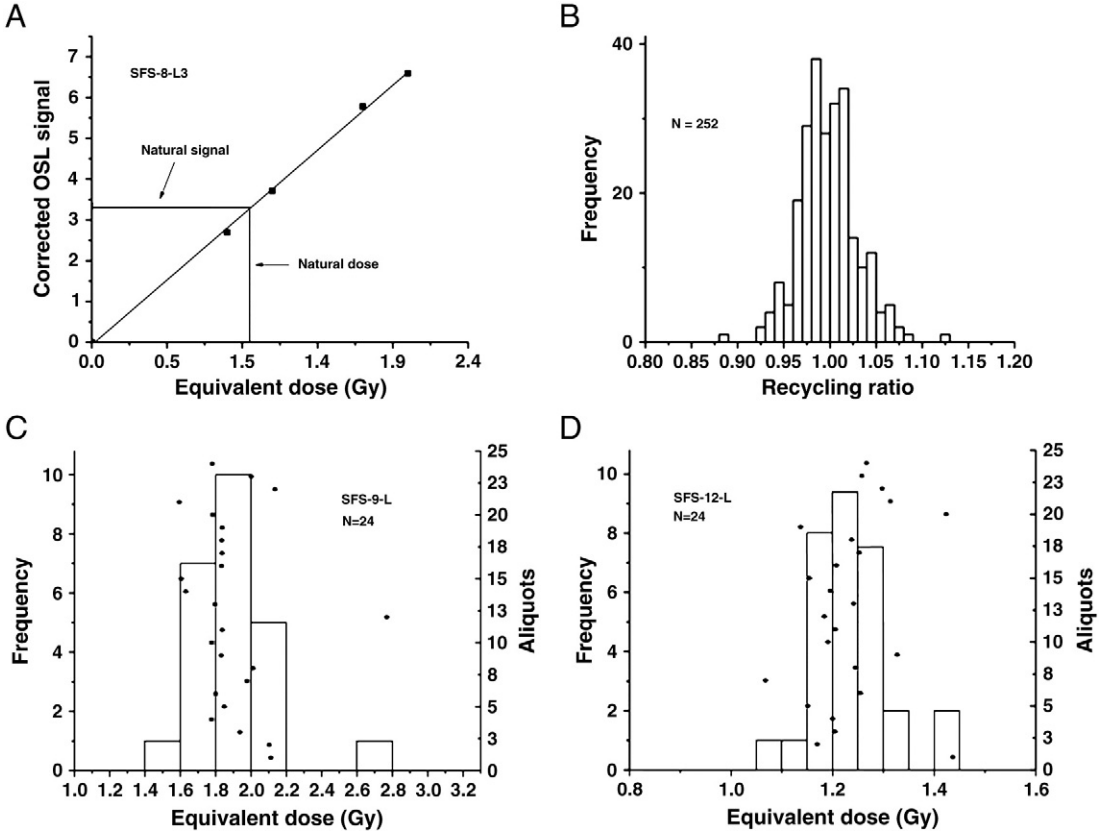

Fig. 6. A) Dose response curve for a quartz aliquot from sample SFS-8-L3. B) Histogram of recycling ratio of 252 aliquots. C and D) Equivalent dose distributions for quartz aliquots samples SFS-9-L and SFS-12-L, respectively. N indicates number of aliquots. Right Y axis indicate the aliquot number.

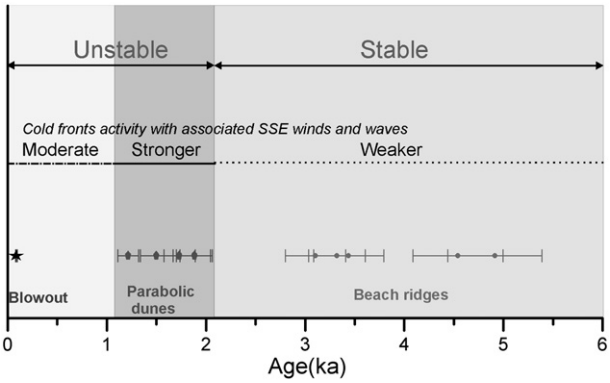

Fig. 7. Beach ridges, parabolic dunes and blowout OSL ages and their relation to cold fronts activity. Unstable and stable periods indicate climatic conditions.

medium to high-grade metamorphic rocks such as kyanite, sillimanite, staurolite and rutile pointing to a primary provenance from source rocks northward of the Itajaí-Açu watershed (Fig. 2B). These sands could be transported directly from the primary source rocks to the SFS barrier through small fluvial systems and alongshore drift or correspond to reworked Pleistocene coastal sediments. The sands deposited under conditions suitable to dune development exhibit a higher concentration of zircon and hornblende, suggesting an elevated input of sediments derived from acid plutonic rocks (Table 3). Acid plutonic rocks dominate the source areas southward of the Itajaí-Açu watershed (Fig. 2B). Heavy minerals assemblages in beach ridges and aeolian dunes show some degree of intermixing between each other.

Rutile, zircon and tourmaline are among the most stable heavy minerals under Earth surface and diagenetic conditions (Hubert, 1962; Morton and Hallsworth, 1999). Although granitic or mafic igneous rocks may be source rocks of rutile, high-grade metamorphic rocks are the most important source of rutile for sediments (Force, 1980), concurrently with recycled sediments. Most igneous rocks lack rutile except where they are hydrothermally altered. Granites, which outcrop in inland areas southward the SFS barrier, present low contents of rutile. Acid igeneous rocks are the main primary sources of zircon. Whereas zircon generally survives the rock cycle from weathering to high grade metamorphism and often even magmatic processes, rutile breakdown occurs at the beginning of the greenschist metamorphic facies and is newly formed at upper amphibolite metamorphic facies conditions (Zack et al., 2004). Zircon and rutile have similar habit (equant or prismatic) and density. The similar hydraulic properties and high stability under the sedimentary cycle make the rutile to zircon ratio (RZi) a robust provenance indicator (Morton and Hallsworth, 1994). For the SFS barrier, the RZi is particularly useful to discriminate sediments derived from the metamorphic and granitic rocks that dominate inland areas of the SFS barrier. The tourmaline to zircon ratio (TZi) would be related to changes in sedimentary reworking due to differences in density between zircon and tourmaline. Sediments with higher degree of reworking would present increased content of zircon grains due to residual concentration by winnowing. Consequently, the TZi would differentiate sedimentary units with variations in the hydraulic conditions responsible for the sediment transport (Guedes et al., 2011a).

In the SFS barrier, heavy minerals content on beach ridges is significantly lower than that showed by aeolian dunes and foreshore (Table 2). Some studies have suggested that heavy minerals concentration in coastal sands is more effective during storm periods (Roy, 1999; Buynevich et al., 2004; Dougherty et al., 2004) and that high velocity aeolian winnowing during low tide periods is an important additional effect (Woolsey et al., 1975). The beach ridges from the SFS barrier are also differentiated by their higher RZi and TZi values (Table 5). The higher RZi values for the beach ridge sands indicate a greater contribution of sediments derived from metamorphic rocks, which is in agreement with a heavy mineral assemblage with elevated contents of staurolite, sillimanite and kyanite. The TZi trend in the SFS barrier is similar to that observed for the RZi, suggesting that it is mainly controlled by provenance. The low values of RZi observed in the parabolic dunes, blowouts, foredunes and present foreshore indicate higher contribution of sediments sourced by the acid plutonic rocks from the Florianopolis batholith located less than 170 km south from the SFS barrier. The Florianópolis batholith (Fig. 2B) is a major component of the northern portion of the Neoproterozoic Dom Feliciano Belt in southern Brazil. The Florianópolis batholith is exposed over an area of about 12,000 km^2 along the coast (Silva et al., 2003) and their sediments reach the coastal systems through coastal watersheds. According to Silva et al. (2003), zircon grains from the Florianópolis batholith are morphologically simple, composed of euhedral long-prismatic crystals with typical magmatic length to width ratio of 3:1. Euhedral zircon grains from the parabolic dunes present a similar length to width ratio (Fig. 5), indicating the input of sediments directly derived from the Florianópolis batholith. Also, this suggests that the sand coarsening from beach ridges to parabolic dunes at around 1891 ± 155 years ago is related to the intensification of the northward litoral drift. Studies by Lessa et al. (2000) at the Paranaguá barrier system (~90 km north of SFS barrier), by Angulo et al. (2009) at the Pontal do Sul barrier (~70 km north of SFS barrier) and by Guedes et al. (2011b) at the Ilha Comprida barrier (~145 km north of SFS barrier), all regions with a

Fig. 8. Foreshore, foredunes and blowouts in the northeastern segment of the SFS barrier (sample site SFS-19-L).

similar geomorphological setting to the SFS barrier, also show changes in progradation during the last two thousand years. In southern Brazil, the northward littoral drift increases during storm conditions. Sand coarsening related to the input of local sediments directly derived from source rocks due to seasonal weather changes was also observed in beach and dune sediments from Kenya (Abuodha, 2003).

5.3. Morphodynamics and provenance changes due to intensification of cold fronts and precipitation in southern Brazil

The Holocene progradation of the SFS barrier had a pronounced morphodynamic shift around 1891 ± 155 years ago, which is the minimum age for triggering dune building. This shift is characterized by changes in barrier morphology due to dune development through stronger SSE winds and alternative sediment provenance combined with sand coarsening. Dune development favored barrier aggradation and decreasing rate of progradation. The relative sea level has fallen at a constant low rate (Angulo et al., 2006) since the progradation of the SFS barrier. At this low rate of relative sea-level change, the influence of sea-level variation in progradation is weakened and the sediment supply to the Holocene barriers from southern Brazil becomes highly sensitive to changes in the wind and wave climate (Sawakuchi et al., 2008). Grain size and heavy minerals indicate that dune development occurred under higher wave energy and increased sediment supply from southern coastal sectors. Fine sand deposition which dominates the SFS barrier evolution until 1891 ± 155 years ago is usually associated with a dissipative morphodynamic beach system (Short and Hesp, 1982) but with insufficient prevailing onshore winds to develop aeolian depositional landforms. No concurrent deposition of beach ridges and aeolian dunes are found on SFS barrier prior to 1891 ± 155 years ago, indicating lack of regular strong winds at the beach ridge progradation stage. Conversely, medium to coarse sand are usually associated with an intermediate or reflective morphodynamic beach system, which would in most cases hinder dune building (Short and Hesp, 1982). However, dune formation in the SFS barrier marks a shift from dissipative to intermediate-reflective beach system. Despite the increase in wave energy favoring a dissipative beach system, the input of medium to coarse sand forced an intermediate-reflective high energy beach system. Also, the increase in heavy minerals concentration from the beach ridges to the dune ridges and present foreshore supports the intensification of storminess since around 1891 ± 155 years ago. The stabilization of parabolic dunes at about 1215 ± 105 years ago and the formation of blowouts and foredunes attest to a relative reduction in regular wind activity. However, wind activity after 1215 ± 105 years ago still persisted more intense than during the beach ridges stage. Therefore, the morphodynamic shift observed in the SFS barrier is a product of Late Holocene climate changes in southern Brazil, which forced intensification of SSE winds and their associated swell wave systems.

In southern Brazilian coast, SSE winds intensify during the northward migration of cold fronts. This is accompanied by increasing in wave height and strengthening of northward littoral drift. Thus, the development of aeolian dunes and augmentation and coarsening of the sediment supply from southern coastal sectors since around 1891 ± 155 years ago mark a change for a phase with more intense cold fronts. This period persisted until at least 1215 ± 105 years ago, when cold fronts activity was reduced, though persisted more intense than before 1891 ± 155 years ago. In southern South America, the period between 1800 and 1200 years ago corresponds to an increase in the amplitude of ENSO events and the seasonal shift of the westerlies storm tracks, poleward in summer and equatorward in winter (Markgraf et al., 2003; Wanner et al., 2008). Sedimentological evidence from Lago Cardiel (Argentina) reveals a higher westerlies wind activity between 1800 and 1200 cal yrs BP (Gilli et al., 2005). This change in the westerlies wind belt is also recorded in marine sediments from Chile (Lamy et al., 2001). Through stable isotopic measurements in biogenic carbonate and bulk organic matter from Lake Guanaco sediments in Chile, Moy et al. (2008) interpreted reduction in amplitude of the westerlies belt starting at the Medieval Climate Anomaly (around AD 950 or 1062 years ago) and terminating at the onset to the Little Ice Age (around AD 1250 or 762 years ago).

The period of parabolic dune formation and stabilization in the SFS barrier coincides with the increasing in precipitation in southern Brazil (Behling, 1995, 1997, 1998; Chiessi et al., 2010). The influence of precipitation on dunefield stabilization during the Mid- to Late-Holocene was found at the Rio Grande do Sul State coastal barriers. According to Martinho et al. (2008), dunefield stabilization in this site occurred from 4820 to 3970 cal yr BP, from 2760 to 2460 cal yr BP and from 1570 to 710 cal yr BP, which are correlated to periods of higher precipitation. Increased storm activity associated with more intense cold fronts is also observed in the Ilha Comprida barrier located 145 km north of the SFS barrier, but dune development induced by SSE winds is observed only during the Little Ice Age (Sawakuchi et al., 2008). Thus, the intensification of cold fronts recorded in the SFS barrier since 1891 ± 155 years ago is also observed in other sectors of southern South America, suggesting that it is a product of changes in the regional climate systems.

The sediment supply for the southern Brazilian barriers originates from minor coastal rivers and from the La Plata River, whose mouth reaches the coast at more than 1000 km south of the SFS barrier. The terrigenous sediments from the La Plata River can be transported northward until the SFS barrier region and even further north (Dominguez, 2006; Mahiques et al., 2008, 2009). However, the bedload from the La Plata River is transported northward through multiple steps of transport and can be stored in southern Brazilian barriers (Sawakuchi et al., 2009). This way of transport dilutes the sediment supply derived from the La Plata River and hinders their contribution to events of abrupt and high inputs of sediments to distal coastal barriers. Contrastingly, nearby local coastal rivers have a fast response to extreme precipitation events, allowing high and sudden inputs of sediments to nearby coastal barriers. The provenance variation observed between the beach ridges and aeolian dunes stages of the SFS barrier record a change from a phase dominated by highly reworked sediments to a phase controlled by the input of sediments derived from southern coastal sectors in the Florianópolis batholith. The main coastal rivers of the SFS barrier region are the Itapacú, Itajaí-Açu, Itajaí-Mirim, Tijucas, Biguaçu and Cubatão Rivers (Fig. 2B). The Itajaí-Açu River basin is the main watershed draining the Florianópolis batholith region. Climatic events like ENSO induce higher discharges of watersheds reaching the southern Brazilian coast, including the Itajaí-Açu River basin (15,500 km^2). Schettini (2002) reports water discharge peak of 5390 m^3/s during the 1984 ENSO event in the Itajaí-Açu River, which greatly surpasses the 1934–1998 average daily discharge of 228 m^3/s. Although ENSO conditions started after 6–5 ka (Rodbell et al., 1999), their intensification is more pronounced during the Late Holocene (van Breukelen et al., 2008) possibly linked with a northbound displacement of the westerlies wind belt (Lamy et al., 2010).

Therefore, the rising of the sediment supply derived from the Florianópolis batholith since 1891 ± 155 years ago could result from increasing precipitation in coastal watersheds south of the SFS barrier due to ENSO intensification combined with stronger northward littoral drift related to the strengthening of cold fronts provoked by a northward migration of the westerlies wind belt (Fig. 7).

6. Conclusions

A pronounced morphodynamic shift occurred in the SFS barrier at around 1891 ± 155 years ago. This shift is characterized by parabolic dunes development and change in sand provenance that indicate conditions of stronger northward littoral drift and SSE winds controlled primarily by enhancement of cold fronts and precipitation in local coastal watersheds. These Late Holocene climate changes in southern Brazilian coast could result from a northbound shift of the

westerlies wind belt coupled with the intensification of ENSO events. These climate forcings on the coastal depositional system generated great changes in barrier morphology, sediment texture and composition and beach morphodynamics. Geomorphological surveys combined with provenance indicators, grain size analysis and OSL dating allowed to assess the impacts of centennial to millennial climate changes on coastal settings. Understanding the link between climate events and coastal processes during the Late Holocene may help evaluating the response of coastal zones to future climate changes.

Acknowledgments

The authors would like to thank Dra. Nancy Kuniko Umisedo for providing the use of the OSL/TL reader of the Dosimetry Laboratory at the Institute of Physics (USP) and Jordana Acuña Zampelli and Elaine Sinfrônio for the support during grain size analysis and heavy mineral separation in the Laboratory of Sedimentology at the Institute of Geosciences (USP). The authors are also grateful to the helpful suggestions made by the editor John T. Wells and the thoughtful comments by two anonymous reviewers which greatly improved the manuscript.

References

Abuodha, J.O.Z., 2003. Grain size distribution and composition of modern dune and beach sediments, Malindi Bay coast, Kenya. Journal of African Earth Sciences 36, 41–54.
Adamiec, G., Aitken, M.J., 1998. Dose-rate conversion factors: update. Ancient TL 16, 37–50.
Aitken, M.J., 1998. An Introduction to Optical Dating. Oxford University Press . (267 pp.).
Alves, J.H.G.M. 1996. Refração do espectro de ondas oceânicas em águas rasas: Aplicações à região costeira de São Francisco do Sul, SC. Dissertação de Mestrado, Engenharia Ambiental, UFSC, Florianópolis. 89p.
Amin Jr., A.H., Dillenburgb, S.R., 2010. Variações das propriedades granulométricas da barreira costeira da Pinheira (SC) durante a sua progradação no Holoceno Superior. Quaternary and Environmental Geosciences 02, 25–39.
Angulo, R.J., Lessa, G.C., 1997. The Brazilian sea-level curves: a critical review with emphasis on the curves from the Paranaguá and Cananéia regions. Marine Geology 140, 141–166.
Angulo, R.J., Souza, M.C., Reimer, P., Sasaoka, S.K., 2005. Reservoir effect of the southern and southeastern Brazilian coast. Radiocarbon 47, 1–7.
Angulo, R.J., Lessa, G.C., Souza, M.C., 2006. A critical review of mid- to late-Holocene sea-level fluctuations on the eastern Brazilian coastline. Quaternary Science Reviews 25, 486–506.
Angulo, R.J., Lessa, G.C., Souza, M.C., 2009. The Holocene Barrier Systems of Paranaguá and Northern Santa Catarina Coasts, Southern Brazil. In: Dillenburg, S.R., Hesp, P. (Eds.), Geology of the Brazilian Coastal Barriers: Lecture Notes in Earth Sciences. Springer-Verlag (380 pp.).
Anthony, E.J., Mrani-Aloui, M., Héquette, A., 2010. Shoreface sand supply and mid- to late Holocene aeolian dune formation on the storm-dominated macrotidal coast of the southern North Sea. Marine Geology 276, 100–104.
Basei, M.A.S., Siga, O.J., Machiavelli, A., Mancini, F., 1992. Evolução tectônica dos terrenos entre os cinturões Ribeira e Dom Feliciano. Revista Brasileira de Geociências 22, 216–221.
Bauer, B.O., 1991. Aeolian Decoupling of Beach Sediments. Annals of the Association of American Geographers 81, 290–303.
Behling, H., 1995. Investigations into the Late Pleistocene and Holocene history of vegetation and climate in Santa Catarina (S Brazil). Vegetation, History and Archaeobotany 4, 127–152.
Behling, H., 1997. Late Quaternary vegetation, climate and fire history from the tropical mountain region of Morro de Itapeva, SE Brazil. Palaeogeography, Palaeoclimatology, Palaeoecology 129, 407–422.
Behling, H., 1998. Late Quaternary vegetational and climatic changes in Brazil. Review of Palaeobotany and Palynology 99, 143–156.
Bristow, C.S., Pucillo, K., 2006. Quantifying rates of coastal progradation from sediment volume using GPR and OSL: the Holocene fill of Guichen Bay, southeast South Australia. Sedimentology 53, 769–788.
Brunn, P., 1962. Sea level rise as a cause of shore erosion. American Society of Civil Engineers Proceedings, Journal Waterways and Harbors Division 88, 117–130.
Buynevich, I.V., FitzGerald, D.M., van Heteren, S., 2004. Sedimentary records of intense storms in Holocene barrier sequences, Maine, USA. Marine Geology 210, 135–148.
Carter, R.W.G., Woodroffe, C.D., 1997. Coastal evolution: Late Quaternary shoreline morphodynamics. Cambridge University Press . (540 pp.).
Chiessi, C.M., Mulitza, S., Pätzold, J., Wefer, G., 2010. How different proxies record precipitation variability over southeastern South America. IOP Conference Series: Earth and Environmental Science 9, 012007.
Clemmensen, L.B., Andreasen, F., Nielsen, S.T., Sten, E., 1996. The late, Holocene coastal dunefield at Vejers, Denmark: characteristics, sand budget and depositional dynamics. Geomorphology 17, 79–98.
Cowell, P.J., Thom, B.G., 1994. Morphodynamics of coastal evolution. In: Carter, R.W.G., Woodroffe, C.D. (Eds.), Coastal Evolution: Late Quaternary Shoreline Morphodynamics. Cambridge University Press, pp. 33–86.
Cooper, J.A.G., Navas, F., 2004. Natural bathymetric change as a control on century-scale shoreline behavior. Geology 32, 513–516.
CPRM. 2004. Carta geológica do Brasil ao milionésimo (1: 1.000.000). Companhia de pesquisa de recursos minerais.
Cruz Jr., F.W., Burns, S.J., Karmann, I., Sharp, W.D., Vuille, M., 2006. Reconstruction of regional atmospheric circulation features during the late Pleistocene in subtropical Brazil from oxygen isotope composition of speleothems. Earth and Planetary Science Letters 248, 494–506.
Cruz Jr., F.W., Burns, S.J., Jercinovic, M., Karmann, I., Sharp, W.D., Vuille, M., 2007. Evidence of rainfall variations in Southern Brazil from trace element ratios (Mg/Ca and Sr/Ca) in a Late Pleistocene stalagmite. Geochimica et Cosmochimica Acta 71, 2250–2263.
Cruz Jr., F.W., Vuille, M., Burns, S.J., Wang, X., Cheng, H., Werner, M., Edwards, R.L., Karmann, I., Auler, A.S., Nguyen, H., 2009. Orbitally driven east–west antiphasing of South American precipitation. Nature Geosciences 2, 210–214.
Dominguez, J.M.L., 2006. The coastal zone of Brazil: an overview. (SI) Journal of Coastal Research 39, 16–20 (Proccendigs of the 8th International Coastal Symposium).
Dougherty, A.J., FitzGerald, D.M., Buynevich, I.V., 2004. Evidence of storm- dominated early progradation of Castle Neck barrier, Massachusetts, USA. Marine Geology 210, 123–134.
Fletcher, M.-S., Moreno, P.I., 2012. Have the Southern Westerlies changed in a zonally symmetric manner over the last 14,000 years? A hemisphere-wide take on a controversial problem. Quaternary International 253, 32–46.
Folk, R.L., Ward, W.C., 1957. Brazos River bar: a study in the significance of grain size parameters. Journal of Sedimentary Petrology 27, 3–26.
Force, E.R., 1980. The provenance of rutile. Journal of Sedimentary Research 50, 485–488.
Galehouse, J.S., 1971. Point Counting. In: Carver, R.E. (Ed.), Procedures in Sedimentary Petrology. Wiley, New York, pp. 385–407.
Gaylord, D.R., Dawson, P.J., 1987. Airflow–terrain interactions through a mountain gap, with an example of eolian activity beneath an atmospheric hydraulic jump. Geology 15, 789–792.
Garreaud, R.D., 1999. Cold air incursions over subtropical and tropical South America: a numerical case study. Monthly Weather Review 127, 2823–2853.
Giannini, P.C.F., Santos, E.R., 1994. Padrões de variação espacial e temporal na morfologia de dunas de orla costeira no centro-sul catarinense. Boletim Paranaense de Geociências 42, 73–96.
Giannini, P.C.F., Sawakuchi, A.O., Martinho, C.T., Tatumi, S.H., 2007. Eolian depositional episodes controlled by Late Quaternary relative sea level changes on the Imbituba–Laguna coast (southern Brazil). Marine Geology 237, 143–168.
Giannini, P.C.F., Guedes, C.C.F., Nascimento Jr., D.R., Tanaka, A.P.B., Angulo, R.J., Assine, M.L., Souza, M.C., 2009. Sedimentology and morphologic evolution of the Ilha Comprida Barrier system, southern São Paulo coast. In: Dillenburg, S.R., Hesp, P. (Eds.), Geology of the Brazilian Coastal Barriers: Lecture Notes in Earth Sciences. Springer-Verlag (380 pp.).
Gilli, A., Arizteguy, D., Anselmetti, F.S., McKenzie, J.A., Markgraf, V., Hajdas, I., McCulloch, R.D., 2005. Mid-Holocene strengthening of the Southern Westerlies in South America — sedimentological evidences from Lago Cardiel, Argentina. Global and Planetary Change 49, 75–93.
Grimm, A.M., Doyle, V.R.B., 2000. Climate variability in South America associated with El Niño and La Niña events. Journal of Climate 13, 35–58.
Guedes, C.C.F., Giannini, P.C.F., Nascimento Jr., D.R., Sawakuchi, A.O., Tanaka, A.P.B., Rossi, M.G., 2011a. Controls of heavy minerals and grain size in a holocene regressive barrier (Ilha Comprida, southeastern Brazil). Journal of South American Earth Sciences 31, 110–123.
Guedes, C.C.F., Giannini, P.C.F., Sawakuchi, A.O., DeWitt, R., Nascimento Jr., D.R., Aguiar, V.A.P., Rossi, M.G., 2011b. Determination of controls on Holocene barrier progradation through application of OSL dating: the Ilha Comprida Barrier example, Southeastern Brazil. Marine Geology 285, 1–16.
Haug, G.H., Hughen, K.A., Sigman, D.M., Peterson, L.C., Rohl, U., 2001. Southward migration of the Intertropical Convergence Zone through the Holocene. Science 293, 1304–1308.
Heil, G. 2006. Abrupt climate shifts in the western tropical to subtropical Atlantic region during the Last Glacial. Dissertation zur Erlangung des Doktorgrades der Naturwissenschaften am Fachbereich Geowissenschaften der Universität Bremen. 121 pp.
Hesp, P., 2002. Foredunes and blowouts: initiation, geomorphology and dynamics. Geomorphology 48, 245–268.
Horn Filho, N.O., Simó, D.H., 2008. The Upper Pleistocene of São Francisco do Sul Island Coastal Plain: geomorphologic, sedimentologic and evolutive aspects. Brazilian Journal of Oceanography 56, 179–187.
Hubert, J.F., 1962. A zircon–tourmaline–rutile maturity index and the interdependance of the composition of heavy mineral assemblages with the gross composition and texture of sandstones. Journal of Sedimentary Petrology 32, 440–450.
Klein, A.H.F., Menezes, J.T., 2001. Beach morphodynamics and profile sequence for a Headland Bay Coast. Journal of Coastal Research 17, 812–835.
Lamy, F., Hebbeln, D., Roehl, U., Wefer, G., 2001. Holocene rain fall variability in southern Chile: a marine record of latitudinal shifts of the Southern Westerlies. Earth and Planetary Science Letters 185, 369–382.
Lamy, F., Kilian, R., Arz, H.W., Francois, J.P., Kaiser, J., Prange, M., Steinke, T., 2010. Holocene changes in the position and intensity of the southern westerly wind belt. Nature Geosciences 3, 695–699.
Lancaster, N., Kocurek, G., Singhvi, A., Pandey, V., Deynoux, M., Ghienne, J.F., Lô, K., 2002. Late Pleistocene and Holocene dune activity and wind regimes in the western Sahara Desert of Mauritania. Geology 30, 991–994.

Lessa, G.C., Angulo, R.J., Giannini, P.C.F., Araujo, A.D., 2000. Stratigraphy and Holocene evolution of a regressive barrier in south Brazil. Marine Geology 165, 87–108.
Madsen, A.T., Murray, A.S., 2009. Optically stimulated luminescence dating of young sediments: a review. Geomorphology 109, 3–16.
Mahiques, M.M., Tassinari, C.C.G., Marcolini, S., Violante, R.A., Figueira, R.C.L., Silveira, I.C.A., Burone, L., Souza, S.H.M., 2008. Nd and Pb isotope signatures on the Southeastern South American upper margin: implications for sediment transport and source rocks. Marine Geology 250, 51–63.
Mahiques, M.M., Wainer, I.K.C., Burone, L., Nagai, R., Souza, S.H.M., Figueira, R.C.L., Silveira, I.C.A., Bícego, M.C., Alves, D.P.V., Hammerb, Ø., 2009. A high-resolution Holocene record on the Southern Brazilian shelf: Paleoenvironmental implications. Quaternary International 206, 52–61.
Markgraf, V., 1998. Past Climates of South America. In: Hobbs, J.E., Lindesay, J.A., Bridgman, H.A. (Eds.), Climates of the Southern Continents: Present, Past and Future. John Wiley and Sons Ltd., pp. 249–264.
Markgraf, V., Bradbury, J.P., Schwalb, A., Burns, S.J., Stern, C., Ariztegui, D., Gilli, A., Anselmetti, F.S., Stine, S., Maidana, N., 2003. Holocene palaeoclimates of southern Patagonia: limnological and environmental history of Lago Cardiel, Argentina (49 S). The Holocene 13, 581–591.
Martin, L., Suguio, K., 1975. The State of São Paulo coastal marine Quaternary geology the ancient strandlines. Anais Academia Brasileira de Ciências 47, 249–263.
Martin, L., Suguio, K., Flexor, J.N., 1988. Hauts niveaux marins pleistocenes du litoral bresilien. Palaeogeography, Palaeoclimatology, Palaeoecology 68, 231–239.
Martinho, C.T., Giannini, P.C.F., Sawakuchi, A.O., 2006. Morphological and depositional facies of transgressive dunefields of the Imbituba-Jaguaruna region, Santa Catarina State, Southern Brazil. (SI) Journal of Coastal Research 39, 673–677 (Proceedings of the 8th International Coastal Symposium).
Martinho, C.T., Dillenburg, S.R., Hesp, P.A., 2008. Mid to late Holocene evolution of transgressive dunefields from Rio Grande do Sul coast, southern Brazil. Marine Geology 256, 49–64.
Milne, G.A., Long, A.J., Bassetta, S.E., 2005. Modelling Holocene relative sea-level observations from the Caribbean and South America. Quaternary Science Reviews 24, 1183–1202.
Moreno, P.I., 2004. Millennial-scale climate variability in northwest Patagonia over the last 15,000 yr. Journal of Quaternary Science 19, 35–47.
Morton, A.C., Hallsworth, C.R., 1994. Identifying provenance-specific features of detrital heavy mineral assemblages in sandstones. Sedimentary Geology 90, 241–256.
Morton, A.C., Hallsworth, C.R., 1999. Processes controlling the composition of heavy mineral assemblages in sandstones. Sedimentary Geology 124, 3–29.
Moy, C.M., Dunbar, R.B., Moreno, P.I., Francois, J.P., Villa-Martinez, R., Mucciarone, D.M., Guilderson, T.P., Garreaud, R.D., 2008. Isotopic evidence for hydrologic change related to the westerlies in SW Patagonia, Chile, during the last millennium. Quaternary Science Reviews 27, 1335–1349.
Murray, A.S., Wintle, A.G., 2000. Luminescence dating of quartz using an improved single-aliquot regenerative-dose protocol. Radiation Measurement 32, 57–73.
Murray-Wallace, C.V., Banerjee, R.P., Bourman, J.M., Olley, J.M., Brooke, B.P., 2002. Optically stimulated luminescence dating of Holocene relict foredunes, Guichen Bay, South Australia. Quaternary Science Review 21, 1077–1086.
Nobre, C.A., Cavalcanti, I.F.A., Gan, M.A., Nobre, P.A., Kayano, M.T., Rao, V.B., Bonatti, J.P., Satyamurti, P., Uvo, C.B., Cohen, J.C., 1986. Aspectos da climatologia dinâmica do Brasil. Climanálise , N° Especial . (65 pp.).
Orford, J.D., Murdy, J.M., Wintle, A.G., 2003. Prograded Holocene beach ridges with superimposed dunes in north-east Ireland: mechanisms and timescales of fine and coarse beach sediment decoupling and deposition. Marine Geology 194, 47–64.
Pezza, A.B., Simmonds, I., 2005. The first South Atlantic hurricane: Unprecedented blocking, low shear and climate change. Geophysical Research Letters 32 (L15712), 1–5.
Possamai, T., Vieira, C.V., Oliveira, F.A., Horn Filho, N.H., 2010. Geologia costeira da ilha de São Francisco do Sul, Santa Catarina. Revista de Geografia 2, 45–58.
Prescott, J.R., Stephan, L.G., 1982. The contribution of cosmic radiation to the environmental dose for thermoluminescence dating. Proceedings of the Second Specialist Seminar on Thermoluminescence Dating, 6. Council of Europe, Strasbourg, pp. 17–25.
Pye, K., 1982. Morphological development of coastal dunes in a humid tropical environment, Cape Bedfordand Cape Flattery, North Queensland. Geografiska Annaler Physical Geography 64, 213–227.
Riccomini, C., Assumpção, M., 1999. Quaternary tectonics in Brazil. Episodes 22, 221–225.
Rodbell, D.T., Seltzer, G.O., Anderson, D.M., Abbot, M.B., Enkeld, D.B., Newman, J.H., 1999. An 15,000-year record of El Niño driven alluviation in Southwestern Ecuador. Science 283, 516–520.
Rodrigues, M.L.G., Franco, D., Sugahara, S., 2004. Climatologia de frentes frias no litoral de Santa Catarina. Revista Brasileira de Geofísica 22, 135–151.
Roy, P.S., 1999. Heavy mineral beach placers in southeastern Australia: their nature and genesis. Economic Geology 94, 567–588.
Sawakuchi, A.O., Kalchgruber, R., Giannini, P.C.F., Nascimento Jr., D.R., Guedes, C.C.F., Umisedo, N.K., 2008. The development of blowouts and foredunes in the Ilha Comprida barrier (Southeastern Brazil): the influence of Late Holocene climate changes on coastal sedimentation. Quaternary Science Reviews 27, 2076–2090.
Sawakuchi, A.O., Giannini, P.C.F., Martinho, C.T., Tanaka, A.P.B., 2009. Grain size and heavy minerals of the Late Quaternary eolian sediments from the Imbituba–Jaguaruna coast, Southern Brazil: depositional controls linked to relative sea-level changes. Sedimentary Geology 222, 226–240.
Schettini, C.A.F., 2002. Caracterização física do estuário do Rio Itajaí-Açu, SC. Revista Brasileira de Recursos Hídricos 7, 123–142.
Seluchi, M.E., Marengo, J.A., 2000. Tropical-midlatitude exchange of air masses during summer and winter in South America: climatic aspects and examples of intense events. International Journal of Climatology 20, 1167–1190.
Short, A.D., Hesp, P.A., 1982. Wave, beach and dune interactions in southeastern Australia. Marine Geology 48, 259–284.
Shulmeister, J., Kirk, R.M., 1993. Evolution of a mixed sand and gravel barrier system in North Canterbury, New Zealand, during Holocene sea-level rise and still-stand. Sedimentary Geology 87, 215–235.
Siga Jr., O., Basei, M.A.S., Machiavelli, A. 1993. Evolução geotectônica da porção NE de Santa Catarina e SE do Paraná, com base em interpretações geocronológicas. Revista Brasileira de Geociências, 23, 215–223. In: Angulo, R. J., Souza, M. C. 2004. Mapa geológico da planície costeira entre o Rio Saí-Guaçu e a Baía de São Francisco, litoral norte do Estado de Santa Catarina. Boletim Paranaense de Geociências 55, 1–20
Silva, L.C., McNaughton, N.J., Hartmann, L.A., Fletcher, I.R., 2003. Contrasting Zircon Growth Patterns in Neoproterozoic Granites of Southern Brazil Revealed by Shrimp U-Pb Analyses and SEM Imaging: Consequences for the Discrimination of Emplacement and Inheritance Ages. Short Papers – IV South American Symposium on Isotope Geology, pp. 689–690.
Siqueira, J.R., Machado, L.A.T., 2004. Influence of the frontal systems on the day-to-day convection variability over South America. Journal of Climate 17, 1754–1766.
Stech, J.L., Lorenzzetti, J.A., 1992. The response of the South Brazil Bight to the passage of wintertime cold fronts. Journal of Geophysical Research 97, 9507–9520.
Stutt, J.B.W., Lamy, F., 2004. Climate variability at the southern boundaries of the Namib (southwestern Africa) and Atacama (northern Chile) coastal deserts during the last 120,000 yr. Quaternary Research 62, 301–309.
Sylvestre, F., 2009. Moisture Pattern During the Last Glacial Maximum in South America. In: Vimeux, F., Sylvestre, F., Khodri, M. (Eds.), Past Climate Variability in South America and Surrounding Regions. Springer-Verlag (418 pp.).
Truccolo, E.C. 1998. Maré meteorológica e forçantes atmosféricas locais em São Francisco do Sul–SC. Dissertação de Mestrado. Departamento de Engenharia Sanitária e Ambiental. Universidade Federal de Santa Catarina. 100pp.
van Breukelen, M.R., Vonholf, H.B., Hellstrom, J.C., Wester, W.C.G., Kroon, D., 2008. Fossil dripwater in stalagmites reveals Holocene temperature and rainfall variation in Amazonia. Earth and Planetary Science Letters 275, 54–60.
Vimeux, F., Ginot, P., Schwikowski, M., Vuille, M., Hoffmann, G., Thompson, L.G., Schotterer, U., 2009. Climate variability during the last 1000 years inferred from Andean ice cores: a review of methodology and recent results. Palaeogeography, Palaeoclimatology, Palaeoecology 281, 229–241.
Wanner, H., Beer, J., Buetikofer, J., Crowley, T.J., Cubasch, U., Flueckiger, J., Goosse, H., Grosjean, M., Joos, F., Kaplan, J.O., Kuettel, M., Mueller, S.A., Prentice, C., Solomina, O., Stocker, T.F., Tarasov, P., Wagner, M., Widmann, M., 2008. Mid- to Late Holocene climate change: an overview. Quaternary Science Reviews 27, 1791–1828.
Wintle, A.G., Murray, A.S., 2006. A review of quartz optically stimulated luminescence characteristics and their relevance in single-aliquot regeneration dating protocols. Radiation Measurements 41, 369–391.
Woolsey, J.R., Henry, V.J., Hunt, J.L., 1975. Backshore heavy-mineral concentration on Sapelo Island, Georgia. Journal of Sedimentary Research 45, 280–284.
Zack, T., Von Eynatten, A., Kronz, A., 2004. Rutile geochemistry and its potential use in quantitative provenance studies. Sedimentary Geology 171, 37–58.